Near-surface Velocity Model Building and Statics in Permafrost Regions

Tianfei Zhu*

CGGVeritas, Calgary AB, Canada

Tianfei.Zhu@cggveritas.com

and

Yan Yan and Jon Downton

CGGVeritas, Calgary AB, Canada

Summary

Near-surface velocity model building represents a major problem in processing of reflection data from permafrost regions because of the strong lateral velocity variations and negative velocity gradients present in these regions. The negative gradients prevent the application of conventional refraction methods in near-surface velocity determination, and the strong lateral variations introduce severe statics anomalies. We show in this study that first-arrival tomography can be used to invert the near-surface structures so long as there are observed turning waves that transverse the low-velocity zones formed by the negative velocity gradients. In the cases where no turning waves are observed, the near-surface structures can be determined by combining first-arrival tomography with reflection tomography.

Introduction

Processing and imaging of reflection data from permafrost regions such as Alaska and the Canadian Arctic are challenging because of the near-surface velocity heterogeneity in these regions. Rapid changes in lithology and water content, together with spatially localized melt zones and ice lakes on the frozen surface, produce extreme lateral velocity variations. Moreover, due to the vertical temperature gradients, these regions often have a high-velocity permafrost surface layer underlain by a low-velocity zone with a negative velocity gradient, preventing the application of conventional refraction methods for velocity determination. In addition to the difficulty of determining the near-surface velocity structure, the strong lateral velocity variations also introduce severe statics anomalies.

Severity of the negative velocity gradient often varies from one area to another. Figure 1 shows three typical sonic logs from permafrost areas. In both cases A and B, velocity below the permafrost layer eventually increases to the permafrost velocity within the logging interval, although the latter well has a much more severe negative gradient and takes a much deeper level to reach the permafrost velocity. Case C, on the other hand, has an extremely severe negative gradient near the surface and the deeper velocity never reaches the permafrost velocity within the
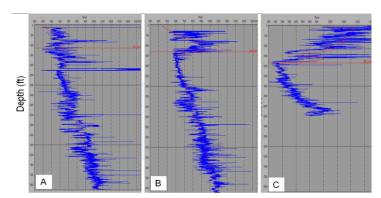

Figure 1: Typical sonic logs from permafrost areas. The red horizontal line indicates the base of permafrost.

logging interval. We show in this study that near-surface velocity structures for case A, and possibly case B, depending on the maximum offset used in the survey, can be determined by a well-implemented first-arrival tomography. First-arrival tomography fails, on the other hand, in case C; near-surface velocity structures in this case must be determined by combining first-arrival tomography with reflection tomography. Even in case C, however, statics calculated by the well-implemented first-arrival tomography can improve stacks significantly as the statics anomalies are usually dominated by extreme lateral variations in a thin layer beneath the surface which can, in some cases, be delineated by the tomography with direct arrivals and scattered waves

First-arrival tomography and negative velocity gradient

Conventional refraction methods represent a velocity structure as constant-velocity layers and treat first arrivals as refraction branches generated along the interfaces between these layers. Each of these refraction branches is described by a linear traveltime segment, and only slopes and intercepts of these traveltime segments are used in calculating the velocity and thickness of each layer. These methods cannot model negative velocity gradients as no refractions will be generated between the two layers with a negative gradient. They may also fail to accommodate strong lateral velocity variations. First-arrival tomography, on the other hand, represents velocity structure by a grid model. Each node of the grid is assigned a velocity and the node velocities can vary in an arbitrary fashion capable of modeling strong velocity variations in both vertical and horizontal directions. Also, first arrivals are now treated as body waves propagating along turning rays. That is, instead of grouped as a few refraction branches, every first arrival is now used as a data point in the tomography to determine the velocity of the nodes traversed by the ray path of this arrival. As a result, layers with a negative velocity gradient within a velocity model can be detected by the first-arrival tomography so long as these layers are traversed by the turning rays of the first arrivals.

Figure 2 is a schematic velocity profile constructed based on the sonic logs A and B in Figure 1 and its corresponding ray diagram. The velocity has a negative gradient between D and E. It then increases again and reaches the value of v(D) at F. The ray diagram shows that the rays beyond receiver R5 will traverse the low-velocity zone DF and eventually turn up as first arrivals at the surface, indicating that the low-velocity zone can be determined by the first arrival tomography. The ray diagram also shows that the low-velocity zone creates a shadow zone on the surface where no turning-wave
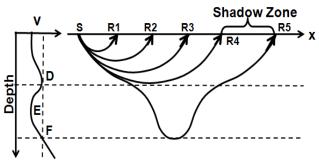

Figure 2: Ray diagram for a velocity profile with a negative gradient.

arrivals are observed. The width of this shadow zone depends on the severity of the negative velocity gradient: The larger the negative gradient is, the wider the shadow zone will be. Thus, long offset data may be required for a survey with a severe negative gradient such as case B in Figure 1 so that first arrivals can be observed at far offsets.

No waves will turn back from the low-velocity zone if the deep velocity is less than the velocity at depth D such as case C in Figure 1. The low-velocity zone in this case can only be calculated using shallow reflections. Even in this case, however, first-arrival tomography plays a key role in determining the velocity structure of a thin layer beneath the surface. This surface layer, as pointed out in the previous section, is extremely heterogeneous and usually cannot be resolved by reflection tomography alone.

The ability of our first-arrival tomography to deal with the permafrost environment is further enhanced by two important features incorporated in our implementation of this technique (Zhu et al., 2000). The traveltimes and ray-paths of first arrivals are calculated by a grid raytracing method (Zhu and Cheadle, 1999). Based on a local wavefront tracking and construction algorithm, this method has been shown to be

highly accurate and robust in modeling turning waves even for extremely heterogeneous media. In addition to turning waves, this method is also capable of modeling scattered waves, a feature especially important for permafrost velocity calculation as some of observed first arrivals are not turning waves but waves generated by scattering due to strong lateral variations. Another feature is that Fresnel-zone effects along a geometric ray are included in our tomographic algorithm. This further enhances the ability of our first-arrival tomography in accurately determining a low-velocity layer.

Examples

Figures 3 and 4 show the near-surface velocity structure from a Canadian Arctic survey obtained by our first-arrival tomography. The survey is a combination of cases A and B described in the previous sections. Figure 3a is the aerial photo image of the survey area, showing the distribution of river channels and ice lakes on the otherwise frozen surface. The survey is located in a coastal region with offshore to the north. Figure 3b shows a depth slice through the derived tomographic model at a depth of 200ft below the surface. Velocities in this slice range from about 12,200 ft/s in the frozen areas (red) to about 5,500ft/s in the offshore melted zone (blue to purple). The pockets and channels delineated by the relatively low-velocity of about 8,400ft/s (green) show an excellent correspondence with the ice lakes and river channels seen in the aerial photo. Figure 4 is a cross section taken from the middle of the model along the north-south direction. It shows the ice lakes diminishing from the surface with depth. The melted zone has a wedge shape
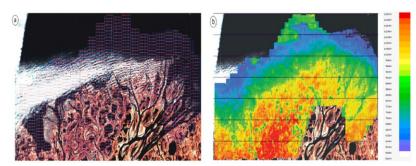

Figure 3: (a) Aerial photo of a permafrost survey area; (b) depth slice through the tomographic model at the depth of 200ft, overlain on the aerial view. Velocity is in ft/s.
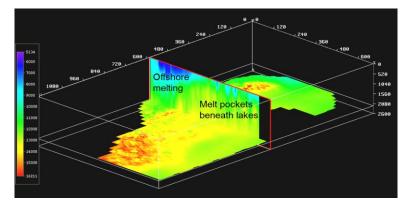

Figure 4: North-south cross section of the velocity model shown in Figure 3. The distance and depth are in feet.

thickening towards offshore, which, if not accounted for, will produce a false long-wavelength structure in stacked sections. Thus, this example shows that first-arrival tomography can indeed be used in cases A and B for determining near-surface velocity structures and for resolving both short and long-wavelength statics anomalies.

A synthetic dataset was used for investigating the velocity model building for case C. The 2D velocity model in Figure 5a represents a transition zone between land and shallow water. Similar to well C in Figure 1, the velocity profile on the left side of the model has a high-velocity permafrost layer with a velocity of 3800m/s at the surface, decreasing to about 3450m/s at the base of the permafrost at about 570m. A low-velocity (about 2200m/s) ice lake is located at the horizontal distance of x=8300m. Right below the permafrost base the velocity drops to 1960 m/s and then increases with depth to about 3100m/s at depth 2300 m. Velocity of the permafrost layer decreases laterally, and the layer submerges below the mixture of ice and water (1950m/s) at shore line x=10000m. This velocity model, together with a constant-layered density model with three interfaces respectively at 800, 1200, and 2000m, was used to generate the

synthetic data with a finite-difference technique. As expected, the first-arrival tomography in this case can only be used to determine velocity of a thin layer beneath the surface. Even in this case, however, the derived velocity layer accurately delineates the ice lake and the transition between land and water
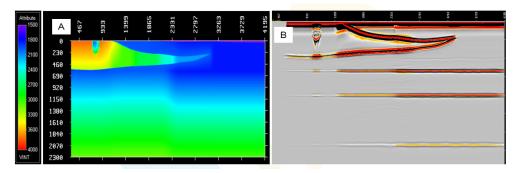

Figure 5: (a) Permafrost model with a high-velocity layer at the surface: (b) its prestack depth image. The distance and depth are in meters.

velocities. To carry out the reflection tomography, we placed this layer atop a smoothly varying velocity model and used this as an initial model for residual curvature analysis (Zhou, et al., 2003). Prestack depth migration was then performed using the final model from this reflection tomography. The migrated section (Figure 5b) shows that both the permafrost layer and density interfaces have been accurately imaged.

Our experiences in processing permafrost datasets have shown that first-arrival tomography often improves long and short-wavelength statics even for case C. This is because the statics anomalies are usually dominated by extreme lateral variations of a thin shallow layer. As demonstrated by the above example, the velocity structure of this shallow layer can, in some cases, be determined by first-arrival tomography using direct arrivals and scattered waves confined within this layer.

Conclusions

We have categorized permafrost regions into three different cases based on the characteristics of their velocity profiles. In cases A and B, where turning waves returning from the bottom and below low-velocity zones are observed, a well-implemented first-arrival tomography is effective in determining their near-surface velocity structures, although a long offset range is required for the latter so that turning waves can be observed at far offsets. In case C, where strong negative velocity gradients prevent turning waves from reaching the recording surface, shallow reflections must be used in combination with first-arrival tomography in near-surface velocity model building.

Our experiences have also shown that first-arrival tomography can improve long and short-wavelength statics even for case C as these anomalies are often dominated by extreme lateral variations of a very shallow layer, which can, in some cases, be delineated by first-arrival tomography with direct arrivals and scattered waves.

Acknowledgements

References

Zhou, H., Gray, S., Yong, J., and Zhang, Y., 2003, Tomographic residual curvature analysis: The process and its components, 73th Annual international Mtg., Soc. Expl. Geophys., Expanded Abstracts, 666-669.

Zhu, T. and Cheadle, S., 1999, A grid raytracing method for near-surface traveltime modeling, 69th Annual international Mtg., Soc. Expl. Geophys., Expanded Abstracts, 1759 – 1763.

Zhu, T., Cheadle, S, Petrella, A., and Gray S. 2000, first-arrival tomography: Method and application, 70th Annual international Mtg., Soc. Expl. Geophys., Expanded Abstracts, 2028-2031.